Direct Laser Writing for Deterministic Lateral Displacement of Submicron Particles

Abdullah T. Alsharhan, Anthony J. Stair, Ruben Acevedo, Talha Razaulla, Roseanne Warren, and Ryan D. Sochol

***Abstract*— Emerging additive manufacturing (or "three-dimensional (3D) printing") strategies offer the potential to vastly extend the capabilities of established microfluidic technologies. For example, the operational performance of "deterministic lateral displacement (DLD)" – a technique in which micro/nanoposts arrayed inside of a microfluidic channel enable passive transport of target suspended particles away from their initial flow streams – is based on geometric design variables, such as the gap spacing between the arrayed posts (*G*). For applications that involve DLD processing of submicron-scale particles (*e.g.*, extracellular vesicles), however, achieving the requisite geometric control *via* conventional microfabrication protocols represents a technically challenging manufacturing hurdle. To bypass such barriers, here we explore the use of two-photon "direct laser writing (DLW)" for additively manufacturing DLD arrays capable of submicron particle handling. Studies of DLW fabrication conditions revealed that increasing the laser power from 22.5 mW to 27.5 mW significantly decreased *G* from 1.51±0.04 μm to 1.02±0.05 μm, respectively. Experimental microfluidic testing of 860 nm-in-diameter fluorescent particles within the DLW-printed DLD system revealed effective hydrodynamic railing of particles along the angled arrayed microposts, with a lateral displacement of 15.3±8.6 μm over a channel length of 500 μm. These results represent, to our knowledge, the first report of a 3D printed DLD system capable of processing submicron particles, thereby offering a promising foundation for DLW-enabled DLD-based biomedical applications. [2020-0123]**

***Index Terms*— 3D printing, additive manufacturing, deterministic lateral displacement, direct laser writing, two-photon polymerization, microfluidics.**

I. Introduction

HISTORICALLY, researchers have primarily employed and/or adapted conventional microfabrication protocols for the production of microfluidic technologies [1]. The associated feature resolutions have provided researchers with a number of scaling-induced benefits (*e.g.*, laminar flow profiles, low reagent volumes, and rapid reaction times) that have proven powerful for biomedical applications including organ modeling [2], diagnostics [3], and drug delivery [4]. One particular example of note is "deterministic lateral displacement (DLD)" – a continuous-flow microfluidic approach for guiding target suspended particles away from their initial laminar flow streams [5]. DLD systems are typically comprised of high numbers of micro/nanoscale posts (or alternatively, pillars) that are arrayed at a slight angle with respect to the flow direction, with the key benefit that the size of displaced particles can be readily customized by modifying basic geometric design parameters that underlie post placement [6], [7].

Motivated by the advantages of DLD – namely, passive and label-free particle processing – many groups have developed DLD arrays to efficiently sort, transport, isolate, and concentrate particles covering a wide range of scales (*e.g.*, DNA, bacteria, and stem cells) [7]–[9]. For designs tailored to submicron particles [10], however, fabricating such DLD devices has demanded increasingly complex manufacturing protocols. In particular, Wunsch *et al*. recently introduced an approach that combined photolithography, reactive-ion etching, e-beam lithography, deep-UV lithography, and glass-Si bonding methods to realize a nanoparticle-based DLD system [11]. Although beneficial for extracellular vesicle [11], [12] and DNA [13] separations, such fabrication processes can be exceedingly time, labor, and cost-intensive, while posing additional training and access-based restrictions associated with equipment and/or facilities requirements [14]. Thus, alternative methodologies for producing DLD systems capable of processing submicron-scale particles are in critical demand.

Over the past decade, researchers have increasingly explored the use of submillimeter-scale additive manufacturing (or colloquially, "three-dimensional (3D) printing") technologies for fabricating microfluidic devices [15], [16], such as using stereolithography [17], [18] and multijet/polyjet printing [19]. Recently, Jusková *et al.* used stereolithography to demonstrate the first 3D printed DLD systems [20], [21]. One caveat, however, is that the minimum size of the target particles was on the order of 20 μm to 120 μm due to the resolution limitations of stereolithography – capabilities that are not suitable for applications that rely on DLD processing of submicron particles [11]–[13]. Consequently, here we investigate the use of "direct laser writing (DLW)" – a two-photon polymerization (2PP)-based additive manufacturing technique with resolutions in the 100 nm range [22]–[24] – for printing DLD systems that target submicron-scale particles.

Manuscript received May 1, 2020; accepted May 24, 2020. This work was supported in part by grants from the US National Science Foundation under Award CMMI-1761395 and Award CMMI-1761273. Subject Editor R. Ghodssi. *(Corresponding author: Ryan D. Sochol.)*

Abdullah T. Alsharhan, Anthony J. Stair, Ruben Acevedo, and Ryan D. Sochol are with the Department of Mechanical Engineering, University of Maryland, College Park, MD 20742 USA (e-mail: rsochol@umd.edu).

Talha Razaulla and Roseanne Warren are with the Department of Mechanical Engineering, The University of Utah, Salt Lake City, UT 84112 USA.

Color versions of one or more of the figures in this article are available online at http://ieeexplore.ieee.org.

Digital Object Identifier 10.1109/JMEMS.2020.2998958

II. Concept

In this work, we present a novel DLW-based manufacturing strategy for DLD array fabrication. Previously, we introduced "*in situ* DLW (*is*DLW)" strategies for printing microfluidic structures directly inside of (and fully sealed to) enclosed microchannels comprising polydimethylsiloxane (PDMS) [25] and the thermoplastic, cyclic olefin polymer (COP) [26]. These studies revealed that COP is far superior as a substrate for direct attachment of DLW-printed features compared to PDMS [24]–[26]. Unfortunately, the optical properties of a bottom substrate (*e.g.*, glass or COP) can slightly diminish the resolution and repeatability of DLW – particularly with respect to height-based power variations [26] – to a degree that would compromise the precision required for submicron particle-based DLD arrays. To bypass such issues, here we instead utilize an unenclosed COP microchannel, with a liquid-phase photomaterial dispensed such that it completely fills the entirety of the microchannel (Fig. 1a).

Using a Dip-in Laser Lithography (DiLL) configuration in which the objective lens of the laser is immersed in the photomaterial, the DLD array is defined *via* selective photopolymerization events. Specifically, a tightly focused femtosecond pulsed IR laser is scanned point-by-point, layer-by-layer to induce localized 2PP in designed locations, first defining the boundaries to the DLD array (fully sealed to the COP walls), and then printing the arrayed posts (Fig. 1b). Due to the precision afforded by the DLW printer, the DLD microstructures can be fabricated such that the height of the COP microchannel and the DLD array are effectively identical. As a result, once the print has been developed, a thin COP film can be permanently bonded to both the COP microchannel as well as the tops of the DLW-printed microstructures, thereby completely sealing the microfluidic device (Fig. 1c).

The fundamental design parameters for DLD arrays include the gap spacing between the posts (G) and the angle of the post array with respect to the flow direction (θ) [5]. The critical diameter D_C – *i.e.*, the minimum particle size that will be passively displaced or "railed" along the arrayed microposts [27], [28] – can be calculated using an empirical model [29]:

$$D_C = 1.4G \times tan(\theta)^{0.48} \quad (1)$$

Although the height of the posts (H) is not included in Eq. 1, increasing H improves the potential throughput of a given DLD array design [21]. Unfortunately, larger H can also lead to stiction-based failure modes for densely packed microposts. To prevent such issues while setting H to be much larger than the diamond-shaped posts (3.5 μm × 3.5 μm) [30], we leveraged the geometric versatility of DLW to construct horizontal support structures (*i.e.*, perpendicular to H) that reinforce the microposts at their midpoints (for $H = 22$ μm) (Fig. 1d). The support structures (diameter = 2 μm) connect the microposts along θ as well as perpendicular to the flow direction. These conditions are designed to promote a consistent G throughout the array while limiting the potential for the support structures to interfere with the capacity for the DLD system to effectively rail the suspended particles away from their original flow streams (Fig. 1d).

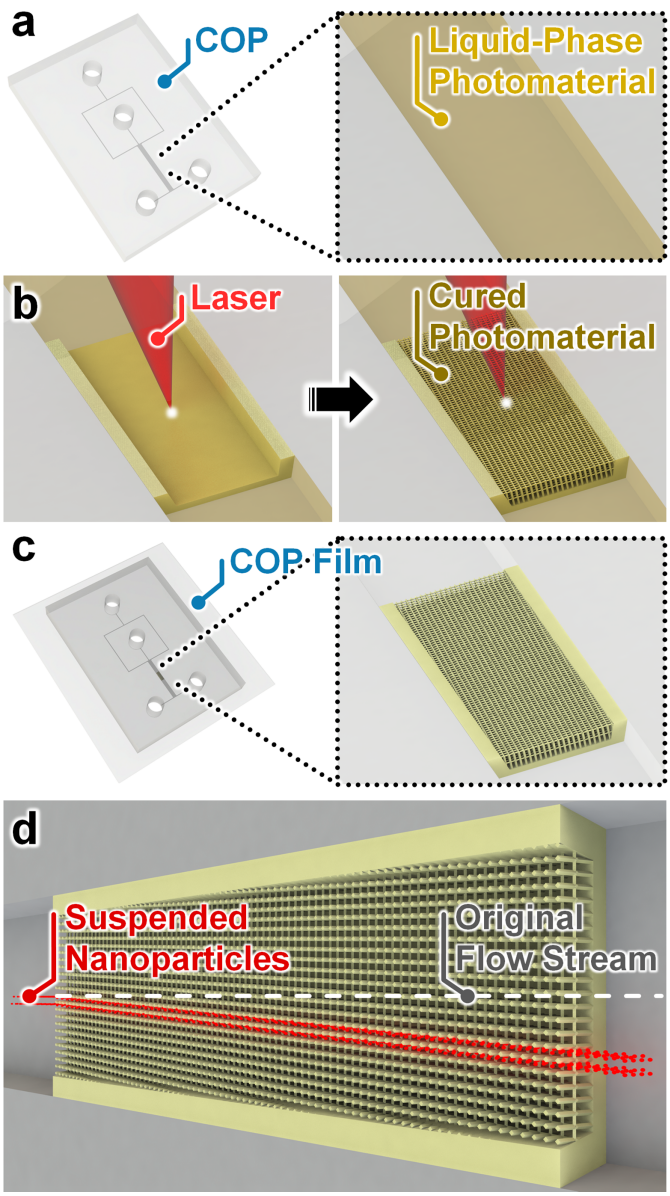

Fig. 1. Conceptual illustrations of the "direct laser writing (DLW)"-based methodology for additively manufacturing "deterministic lateral displacement (DLD)" arrays. (a) Micropatterned cyclic olefin polymer (COP) with an expanded view of the unenclosed microchannel filled with a liquid-phase photomaterial. (b) The DLW process for printing the boundaries of the DLD fully adhered to the COP channel walls (*left*), and then the DLD microstructures (*right*). (c) The sealed DLD microfluidic device following solvent-based bonding of a thin COP film to the micropatterned COP with embedded DLD array. (d) Under continuous-flow conditions, the DLD system passively rails target suspended nanoparticles along the posts (arrayed at an angle with respect to the flow direction), away from their initial flow streams.

III. Materials and Methods

A. Cyclic Olefin Polymer (COP) Microchannel Fabrication

To manufacture the unenclosed COP microchannel, we employed a previously reported DLW-based method for COP-based microreplication [26]. Briefly, the microchannel molds were modeled using the computer-aided design (CAD)

software, SolidWorks (Dassault Systemes, France), exported as STL files, and then imported into the computer-aided manufacturing (CAM) software, DeScribe (Nanoscribe, Karlsruhe, Germany), for slicing and laser writing path generation. It is important to note that the microchannel geometry corresponding to the location of the eventual DLD array was designed with a trapezoidal cross-section to prevent print failures along the side walls [24]–[26].

A Si substrate (25 mm × 25 mm) was rinsed with acetone and isopropyl alcohol (IPA), and then dried with N_2 gas before being place on a 100 °C hot plate for 15 min. A drop of IP-S photoresist (Nanoscribe) was dispensed onto the Si substrate, which was then loaded into the Nanoscribe Photonic Professional GT printer in the DiLL configuration for DLW of the negative mold using a 25× objective lens. After the DLW process, the substrate was developed using propylene glycol monomethyl ether acetate (PGMEA) and IPA, and then dried with N_2 gas. A 4-mm-thick COP sheet (ZEONOR 1060R, Zeon Corp., Japan) was rinsed with IPA and dryed with N_2 gas. Using the printed negative master mold, the patterns were replicated onto the COP sheet *via* hot embossing for 3 min at 120 °C. Afterward, ports were drilled at inlet/outlet locations.

B. Direct Laser Writing (DLW) of the Deterministic Lateral Displacement (DLD) Array

Similar to the unenclosed COP microchannel, the DLD array design was modeled in SolidWorks and imported into DeScribe for fabrication with the Nanoscribe DLW printer. An aliquot of IP-Dip photoresist (Nanoscribe) was dispensed directly onto the unenclosed COP microchannel – *i.e.*, fully covering the intended location of the DLD array – and then loaded into the Nanoscribe printer in the DiLL configuration for DLW of the DLD structures using a 25× objective lens. The unenclosed DLD array was developed using PGMEA and IPA, and then dried with N_2 gas.

C. Solvent-Based COP Bonding

To achieve a fully enclosed microfluidic system, we employed a solvent-based bonding process [26] using cyclohexane solvent. A thin COP film (microfluidic ChipShop GmbH, Germany) was exposed to cyclohexane vapor at 30 °C for approximately 2 min. Directly after the vapor exposure process, the exposed surface of the COP film was brought into contact with the unenclosed surface of the micropatterned COP (and embedded DLD array) to facilitate a permanent bond, thereby fluidically sealing the device.

D. Experimental Characterization

Optical characterizations *via* scanning electron microscopy (SEM) were performed using a TM4000 Tabletop SEM (Hitachi, Tokyo, Japan). Microfluidic experiments were conducted using Fluigent Microfluidic Control System (MFCS) and flow rate platforms along with MAESFLO software (Fluigent, France). Two input solutions/suspensions were prepared for microfluidic testing: (*i*) a buffer solution comprised of DI water and 1% (v/v) Tween 20 (MilliporeSigma, St. Louis, USA), and (*ii*) a nanoparticle suspension comprised of DI water, 1% (v/v) Tween 20, and 0.01% (v/v) 860 nm fluorescent polystyrene particles (Thermo Fisher Scientific, Waltham, USA). The

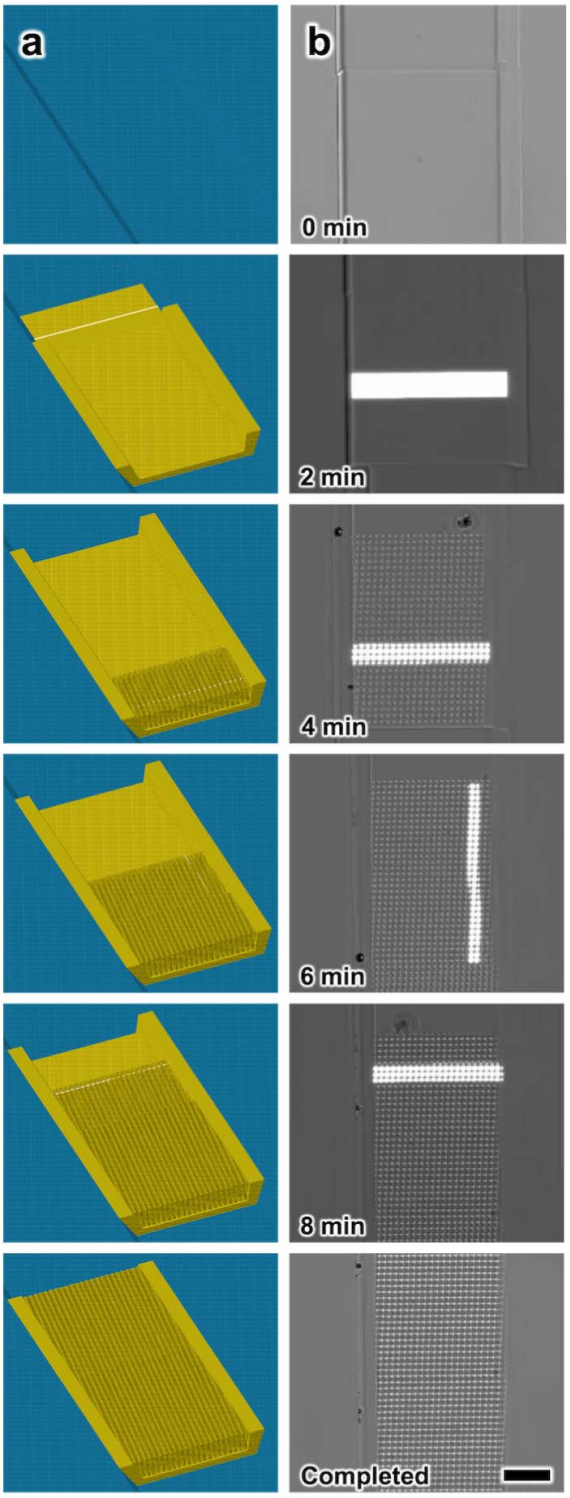

Fig. 2. Fabrication results for DLW-based printing of a DLD array (800 μm in length) in an unenclosed COP microchannel (30 μm in height). (a) Computer-aided manufacturing (CAM) simulations and (b) corresponding micrographs of the DLW printing process. Total print time ≈ 9 min; Scale bar = 50 μm.

distinct fluidic samples were inputted into the microfluidic chip using fluorinated ethylene propylene tubing (Cole-Parmer, Vernon Hills, IL) and stainless-steel couplers (20 ga., Instech, Plymouth Meeting, PA). Fluorescence results were obtained *via* an inverted fluorescence microscope (Axio Observer.Z1, Zeiss, Germany) connected to a charge-coupled device (CCD) camera (Axiocam 503 Mono, Zeiss). To quantify the magnitude of lateral displacement, time-lapse fluorescence micrographs were processed using ImageJ (NIH, Bethesda, MD) to measure the mean-to-mean and peak-to-peak shifts in fluorescence intensity corresponding to the paths of the flowing suspended fluorescent particles: (*i*) directly prior to entering the DLD array, and (*ii*) directly after exiting the DLD array. Results in the text are presented as mean ± standard deviation.

IV. Results and Discussion

A. DLW-Based DLD Array Fabrication

CAM simulations and corresponding micrographs of the fabrication results for DLW-based printing of an 800-μm-long DLD array (comprised of four adjacently printed segments) directly inside of an unenclosed trapezoidal COP microchannel are presented in Fig. 2a and 2b, respectively. Among the geometric design variables that govern the size of particles that can be railed using DLD (Eq. 1), G is particularly susceptible to unintended variations due to DLW process conditions. Specifically, the size of the 2PP point (or "voxel") can be modified by adjusting either the laser power or the scanning speed. In this study, we set the scanning speed to remain constant at 10 mm/s (*i.e.*, to ensure consistency with prior work [26], [31]) and investigated the effects of varying laser power on G. Fabrication results for identically designed DLD arrays ($G = 1$ μm), but varying laser power revealed that lower laser powers produced smaller microposts, and thus, significantly larger G ($p < 0.01$) (Fig. 3a). For example, DLD arrays printed with laser powers of 22.5 mW, 25 mW, and 27.5 mW yielded average G of 1.51±0.04 μm (Fig. 3a – *i*), 1.21±0.04 μm (Fig. 3a – *ii*), and 1.02±0.05 μm (Fig. 3a – *iii*), respectively. These results suggest that a laser power of 27.5 mW produced DLD arrays that closely matched those of the original design. With respect to Eq. 1, we found that applying an incorrect laser power could lead to unintended alterations of D_C. By selecting a laser power corresponding to designed DLD geometric parameters, we observed that DLW could be effectively employed for DLD array manufacturing (*e.g.*, Fig. 3b).

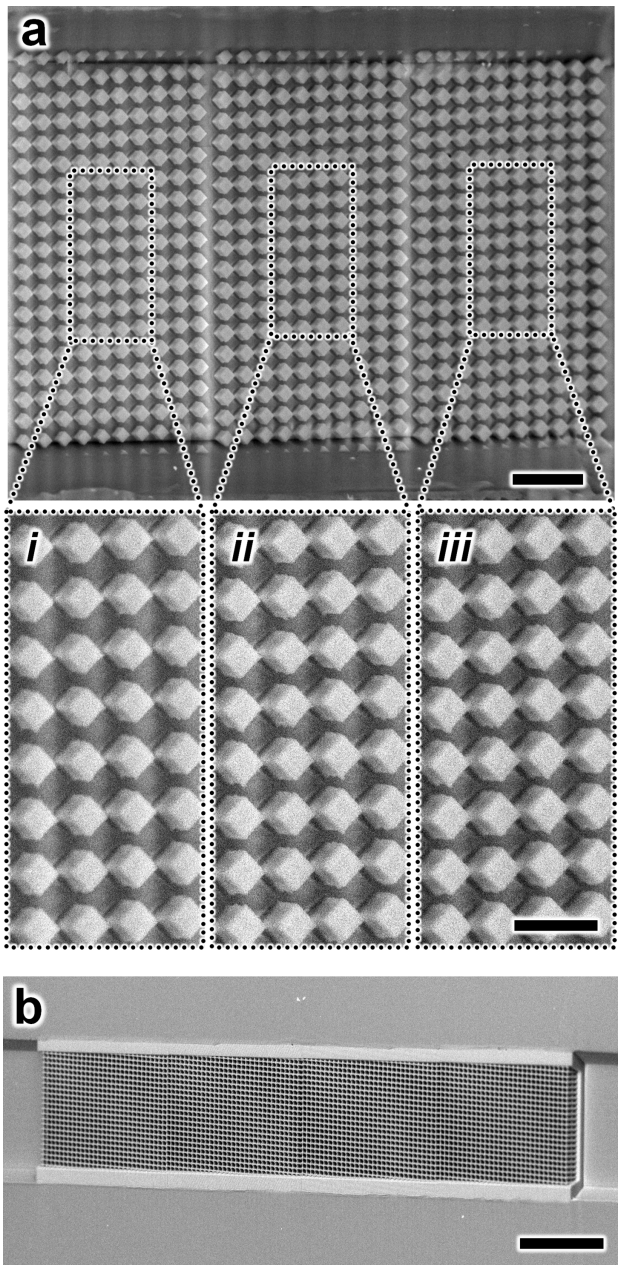

Fig. 3. SEM micrographs of DLW fabrication results. (a) Three identically designed DLD arrays printed using distinct laser powers of: (*i*) 22.5 mW, (*ii*) 25 mW, and (*iii*) 27.5 mW. Scale bars = 20 μm; (*i-iii*) 10 μm. (b) SEM micrograph of a DLW-printed DLD array (800 μm in length) in an unenclosed COP microchannel (30 μm in height). Scale bar = 100 μm.

B. DLD of Submicron Particles

To evaluate the core functionality of the DLW-printed DLD array, we performed continuous-flow microfluidic experiments with submicron fluorescent polystyrene particles (860 nm in diameter) and monitored particle displacement behaviors under fluorescence microscopy. For microfluidic testing, we fabricated a DLD system (180 μm in width; 500 μm in length) inside of a 200-μm-wide and 30-μm-high COP microchannel that comprised diamond-shaped microposts (3.5 μm × 3.5 μm; $h = 22$ μm) arrayed with G of 2.5 μm and θ of 0.05 radians (Fig. 4a). These DLD array design parameters correspond to a D_C of 831 nm (Eq. 1), which satisfies the condition of being adequately smaller than the size of the target 860 nm particles. To prevent undesired particle-side wall interactions (*i.e.*, boundary effects) that can compromise DLD phenomena [6], we inputted a buffer solution distributed to both sides of the particle suspension channel, thereby hydrodynamically focusing the particle stream toward the center of the microchannel before entering the DLD array (Fig. 4b).

Fluorescence imaging during microfluidic experimentation revealed several key results. First, consistent with prior DLD

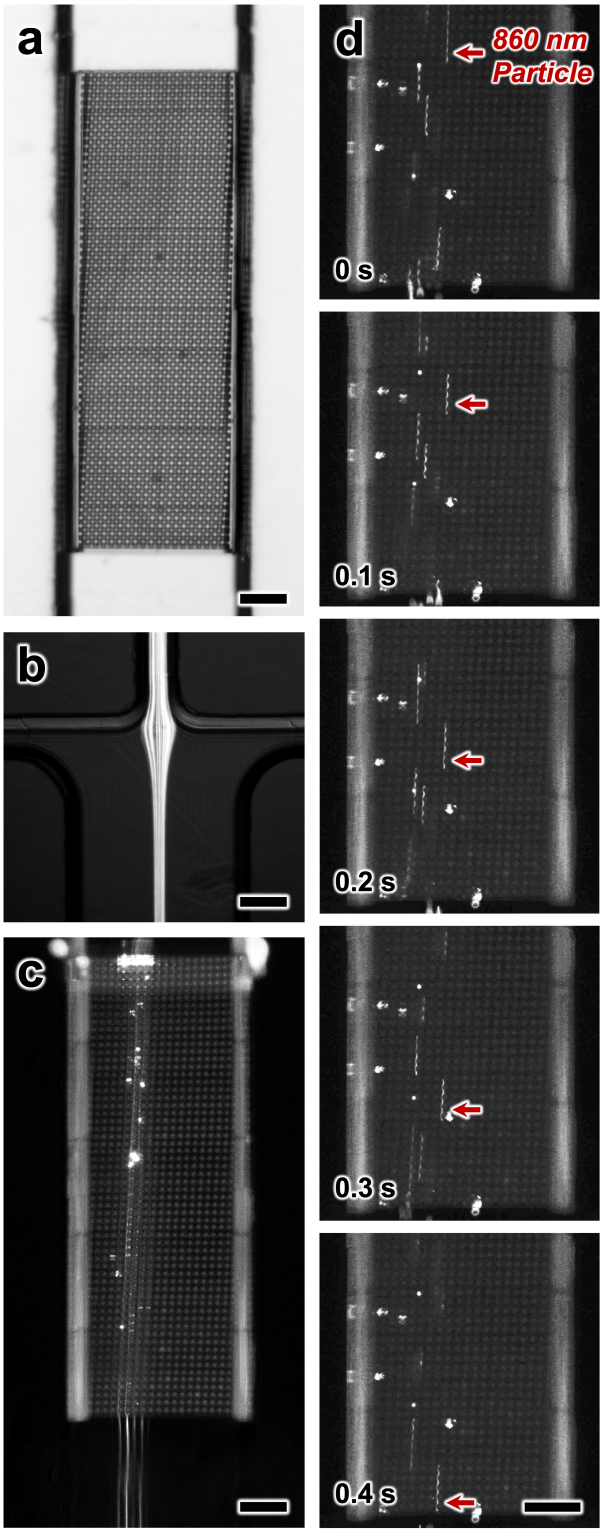

Fig. 4. Experimental results for microfluidic DLD of 860 nm fluorescent polystyrene particles. (a) Brightfield image of the DLW-printed DLD array. (b) Input microchannels corresponding to the particle suspension (*middle*) and buffer solution (*left*; *right*). (c) Time-lapse fluorescence micrograph of particle streams through the DLD array. (d) Sequential fluorescence micrographs during particle transport through the DLD array. Scale bars = 50 μm.

works [11], [32], we observed a degree of particle clogging at the entrance of the DLD array, as evidenced by the increased fluorescence intensities corresponding to the pathway of the particles flowing into the array (Fig. 4c). One potential basis for this result is the occurrence of particle agglomeration prior to microfluidic loading, resulting in adherent sets of particles with effective diameters that are larger than G. Although the surfactant, Tween 20, was included in the particle suspension (as well as the buffer solution) to preclude such issues, it is possible that some agglomeration persisted. The inclusion of additional particle filters prior to the DLD entryway could further limit such clogging events in the DLD array. Nonetheless, we found that suspended particles were able to bypass the initial clogging region, continuously flowing directly through this area and then the full DLD array (Fig. 4c,d). It is likely that the larger H contributed to the ability for mobile suspended particles to circumvent immobilized ones (*e.g.*, entering the DLD array at different heights to avoid the clogging events).

To evaluate the efficacy of the DLW-printed DLD array in guiding the target 860 nm particles away from their initial flow streams, we quantified the changes in fluorescence intensity characteristics – a measure of the trajectories of suspended particles (*e.g.*, Fig. 4d) during their transport through the microfluidic system – preceding and succeeding the DLD array. The quantified experimental results for particle flow behavior corresponding to the 500-μm-long DLD array revealed mean-to-mean and peak-to-peak shifts suggesting lateral displacements of 15.3±8.6 μm and 16.3±8.9 μm, respectively. In combination, the experimental results demonstrate that the presented DLW-based approach is suitable for fabricating DLD arrays capable of processing submicron particles.

V. Conclusion

State-of-the-art additive manufacturing technologies hold promise for advancing a diversity of microfluidic systems. In this work, we explored the use of DLW for 3D printing DLD arrays at scales that enable hydrodynamic processing of submicron particles. To do so, we presented a novel manufacturing methodology that entailed DLW-printing DLD arrays in unenclosed COP microchannels and then fluidically sealing the devices *via* solvent-bonding processes. DLW fabrication results revealed a critical role for laser power in controlling G, with an approximately 22% increase in laser power resulting in a 48% decrease in G and a demonstrated resolvable G as low as 1.02±0.05 μm. Microfluidic experimentation with 860 nm particles revealed successful lateral displacements quantified as 15.3±8.6 μm (mean-to-mean) and 16.3±8.9 μm (peak-to-peak) over a 500-μm-long DLW-printed DLD array. These results suggest that the presented strategy could be expanded to mixed suspensions with varying particle size ranges for sorting, isolation, and/or purification-based DLD applications.

Although the DLD design used for transporting 860 nm particles included G of 2.5 μm and a θ of 0.05 radians, these geometric parameters can be readily modified to tailor D_C (Eq. 1) for desired applications (*e.g.*, D_C < 250 nm *via* the lowest G demonstrated in this work and θ = 0.025 radians). Similarly, the reported DLD array was designed with H of 22 μm; however, we envision that the presented methodology could be extended to DLW-print DLD systems with significantly larger H to yield high throughput capabilities [21] or gravity driven adaptations [33]. As prior works have reported that

modifying the shape of monolithic DLD posts can improve particle sorting efficiencies [30], [34], [35], the architectural versatility inherent to DLW could be leveraged to support 3D investigations of such concepts. Nonetheless, the present study serves as a fundamental proof of concept for the use of DLW for DLD array fabrication, while also marking the first report of a 3D printed DLD system capable of processing submicron-scale particles (to our knowledge). Extensions of this DLW-based strategy offer potential to advance numerous DLD-based biomedical research and applications that involve particles at smaller scales.

Acknowledgment

The authors would like to thank the contributions of R. Utz, A. Lamont, M. Restaino, and the members of the Bioinspired Advanced Manufacturing (BAM) Laboratory. They would also like to thank the help and support of technical staff and members of Terrapin Works at the University of Maryland, College Park.

References

[1] E. K. Sackmann, A. L. Fulton, and D. J. Beebe, "The present and future role of microfluidics in biomedical research," *Nature*, vol. 507, no. 7491, pp. 181–189, Mar. 2014.

[2] A. Sontheimer-Phelps, B. A. Hassell, and D. E. Ingber, "Modelling cancer in microfluidic human organs-on-chips," *Nature Rev. Cancer*, vol. 19, no. 2, pp. 65–81, Feb. 2019.

[3] W. Yu *et al.*, "A ferrobotic system for automated microfluidic logistics," *Sci. Robot.*, vol. 5, no. 39, Feb. 2020, Art. no. eaba4411.

[4] A. C. Daly, L. Riley, T. Segura, and J. A. Burdick, "Hydrogel microparticles for biomedical applications," *Nature Rev. Mater.*, vol. 5, pp. 20–43, Nov. 2019.

[5] L. R. Huang, "Continuous particle separation through deterministic lateral displacement," *Science*, vol. 304, no. 5673, pp. 987–990, May 2004.

[6] J. McGrath, M. Jimenez, and H. Bridle, "Deterministic lateral displacement for particle separation: A review," *Lab Chip*, vol. 14, no. 21, pp. 4139–4158, 2014.

[7] S.-C. Kim, B. H. Wunsch, H. Hu, J. T. Smith, R. H. Austin, and G. Stolovitzky, "Broken flow symmetry explains the dynamics of small particles in deterministic lateral displacement arrays," *Proc. Nat. Acad. Sci. USA*, vol. 114, no. 26, pp. E5034–E5041, Jun. 2017.

[8] Y. Chen *et al.*, "Concentrating genomic length DNA in a microfabricated array," *Phys. Rev. Lett.*, vol. 114, no. 19, May 2015, Art. no. 198303.

[9] M. Xavier *et al.*, "Label-free enrichment of primary human skeletal progenitor cells using deterministic lateral displacement," *Lab Chip*, vol. 19, no. 3, pp. 513–523, 2019.

[10] K. K. Zeming, N. V. Thakor, Y. Zhang, and C.-H. Chen, "Real-time modulated nanoparticle separation with an ultra-large dynamic range," *Lab Chip*, vol. 16, no. 1, pp. 75–85, 2016.

[11] B. H. Wunsch *et al.*, "Nanoscale lateral displacement arrays for the separation of exosomes and colloids down to 20 nm," *Nature Nanotechnol.*, vol. 11, no. 11, p. 936, 2016.

[12] J. T. Smith *et al.*, "Integrated nanoscale deterministic lateral displacement arrays for separation of extracellular vesicles from clinically-relevant volumes of biological samples," *Lab Chip*, vol. 18, no. 24, pp. 3913–3925, 2018.

[13] B. H. Wunsch *et al.*, "Gel-on-a-chip: Continuous, velocity-dependent DNA separation using nanoscale lateral displacement," *Lab Chip*, vol. 19, no. 9, pp. 1567–1578, 2019.

[14] R. D. Sochol *et al.*, "3D printed microfluidics and microelectronics," *Microelectron. Eng.*, vol. 189, pp. 52–68, Apr. 2018.

[15] A. V. Nielsen, M. J. Beauchamp, G. P. Nordin, and A. T. Woolley, "3D printed microfluidics," *Annu. Rev. Anal. Chem.*, vol. 13, Jun. 2020. [Online]. Available: https://www.annualreviews.org/doi/10.1146/annurev-anchem-091619-102649

[16] F. Li, N. P. Macdonald, R. M. Guijt, and M. C. Breadmore, "Increasing the functionalities of 3D printed microchemical devices by single material, multimaterial, and print-pause-print 3D printing," *Lab Chip*, vol. 19, no. 1, pp. 35–49, 2019.

[17] Y.-S. Lee, N. Bhattacharjee, and A. Folch, "3D-printed quake-style microvalves and micropumps," *Lab Chip*, vol. 18, no. 8, pp. 1207–1214, 2018.

[18] H. Gong, A. T. Woolley, and G. P. Nordin, "3D printed selectable dilution mixer pumps," *Biomicrofluidics*, vol. 13, no. 1, Jan. 2019, Art. no. 014106.

[19] R. D. Sochol *et al.*, "3D printed microfluidic circuitry via multijet-based additive manufacturing," *Lab Chip*, vol. 16, no. 4, pp. 668–678, 2016.

[20] P. Juskova, A. Ollitrault, M. Serra, J.-L. Viovy, and L. Malaquin, "Resolution improvement of 3D stereo-lithography through the direct laser trajectory programming: Application to microfluidic deterministic lateral displacement device," *Analytica Chim. Acta*, vol. 1000, pp. 239–247, Feb. 2018.

[21] P. Jusková, L. Matthys, J.-L. Viovy, and L. Malaquin, "3D deterministic lateral displacement (3D-DLD) cartridge system for high throughput particle sorting," *Chem. Commun.*, vol. 56, no. 38, pp. 5190–5193, 2020.

[22] V. Hahn *et al.*, "Rapid assembly of small materials building blocks (Voxels) into large functional 3D metamaterials," *Adv. Funct. Mater.*, Jan. 2020, Art. no. 1907795, doi: 10.1002/adfm.201907795.

[23] J. Lölsberg, A. Cinar, D. Felder, G. Linz, S. Djeljadini, and M. Wessling, "Two-photon vertical-flow lithography for microtube synthesis," *Small*, vol. 15, no. 33, Jun. 2019, Art. no. 1901356.

[24] J. Lölsberg, J. Linkhorst, A. Cinar, A. Jans, A. J. C. Kuehne, and M. Wessling, "3D nanofabrication inside rapid prototyped microfluidic channels showcased by wet-spinning of single micrometre fibres," *Lab Chip*, vol. 18, no. 9, pp. 1341–1348, 2018.

[25] A. C. Lamont, A. T. Alsharhan, and R. D. Sochol, "Geometric determinants of *in-situ* direct laser writing," *Sci. Rep.*, vol. 9, no. 1, pp. 1–12, Dec. 2019.

[26] A. T. Alsharhan, R. Acevedo, R. Warren, and R. D. Sochol, "3D microfluidics via cyclic olefin polymer-based *in situ* direct laser writing," *Lab Chip*, vol. 19, no. 17, pp. 2799–2810, 2019.

[27] R. D. Sochol, S. Li, L. P. Lee, and L. Lin, "Continuous flow multi-stage microfluidic reactors via hydrodynamic microparticle railing," *Lab Chip*, vol. 12, no. 20, pp. 4168–4177, 2012.

[28] R. D. Sochol *et al.*, "Dual-mode hydrodynamic railing and arraying of microparticles for multi-stage signal detection in continuous flow biochemical microprocessors," *Lab Chip*, vol. 14, no. 8, pp. 1405–1409, 2014.

[29] J. A. Davis *et al.*, "Deterministic hydrodynamics: Taking blood apart," *Proc. Nat. Acad. Sci. USA*, vol. 103, no. 40, pp. 14779–14784, Oct. 2006.

[30] K. Loutherback, K. S. Chou, J. Newman, J. Puchalla, R. H. Austin, and J. C. Sturm, "Improved performance of deterministic lateral displacement arrays with triangular posts," *Microfluidics Nanofluidics*, vol. 9, no. 6, pp. 1143–1149, Dec. 2010.

[31] A. T. Alsharhan *et al.*, "A 3D nanoprinted normally closed microfluidic transistor," in *Proc. IEEE 33rd Int. Conf. Micro Electro Mech. Syst. (MEMS)*, Jan. 2020, pp. 131–134.

[32] T. Zhang *et al.*, "Focusing of sub-micrometer particles in microfluidic devices," *Lab Chip*, vol. 20, no. 1, pp. 35–53, 2020.

[33] S. Du and G. Drazer, "Gravity driven deterministic lateral displacement for suspended particles in a 3D obstacle array," *Sci. Rep.*, vol. 6, no. 1, p. 31428, Nov. 2016.

[34] K. K. Zeming, S. Ranjan, and Y. Zhang, "Rotational separation of non-spherical bioparticles using I-shaped pillar arrays in a microfluidic device," *Nature Commun.*, vol. 4, no. 1, pp. 1–8, Jun. 2013.

[35] S. Ranjan, K. K. Zeming, R. Jureen, D. Fisher, and Y. Zhang, "DLD pillar shape design for efficient separation of spherical and non-spherical bioparticles," *Lab Chip*, vol. 14, no. 21, pp. 4250–4262, 2014.